Table 2 Classical Bartter syndrome with growth hormone deficiency: cases from the literature

Reference	Age, years	Sex	Mutation	GH peak (μg/L) to stimulants	IGF-1 (ng/mL)
[9]	5	M	IVS2-1G > C/W610X	9.3 (GLC), 8.0 (CLN), 8.2 (L-DOPA), 38.0 (ARG)	Not determined
[10]	8	F	Not determined	2.9 (INS), 2.0 (CLN), 6.9 (GRF)	122.1
[7]	10	M	Not determined	3.20 (INS), 3.20 (L-DOPA)	25
[8]	10	F	Not determined	0.70 (L-DOPA), 1.96 (CLN)	41.5
	11	M	Not determined	4.70 (L-DOPA), 1.79 (CLN)	39.7
	11	M	Not determined	0.50 (L-DOPA), 4.49 (CLN)	38.3
[2]	11	M	ΔExon1-6/ΔExon1-6	7.6 (ARG)	Low
	14	M	ΔExon1-19/ΔExon1-19	2.4 (ARG), 8.4 (GRF)	Low
[3]	22	F	Not determined	Absence (INS), 8.0 (ARG)	Not determined
Present case	14	M	ΔL130/ΔExon1-3	0.15 (INS), 0.39 (ARG)	80

ARG arginine, *CLN* clonidine, *L-DOPA* L-3,4-dihydroxyphenylalanine, *GH* growth hormone, *GLC* glucagon, *GRF*, growth hormone releasing factor, *IGF-1* insulin-like growth factor 1, *INS* insulin.

hormone (GH) status, and he was found to have profound GHD. His serum levels of IGF-1 and IGF binding protein 3 were 80ng/mL (normal range for his age, 178 to 686ng/mL) and 1.92μg/mL (normal range for his age, 2.69 to 4.16μg/mL), respectively. Pharmacologically stimulated GH levels were 0.15 and 0.39μg/L after insulin-induced hypoglycemia and arginine administration, respectively (Table 1). His bone age was 11.4 years (Tanner-Whitehouse 2-radius, ulna and short bones (TW2-RUS) method for Japanese individuals). Magnetic resonance imaging study results revealed no abnormalities in the hypothalamic-pituitary region (Figure 2).

GH therapy was initiated at 14.5 years of age at a dose of 21 to 27μg/kg/day, which restored his growth remarkably (Figure 1). Although his pubertal stage progressed from Tanner stage 1 to stage 2 over the next two years, his bone maturation (Δbone age/Δchronological age) was 1.02. No significant change was observed in his serum potassium level during GH therapy.

Discussion

To the best of our knowledge, the association of BS with GHD was first reported in 1977 [3]. Thereafter, a number of similar reports have been published [2-8]. However, we believe that some of the older cases reported in the literature do not comply with the current definition and concept of BS and thus should be recognized as GS [4-6]. GS is another salt-losing tubulopathy caused by mutations in the *SLC12A3* gene that encodes the thiazide-sensitive sodium-chloride cotransporter (NCCT) [1]. Because classic BS and GS shared the laboratory finding of hypokalemic alkalosis, these conditions were not strictly discriminated until the era of molecular diagnosis.

Table 3 Gitelman syndrome (including definite or probable cases) and GHD: cases from the literature

Reference	Age, years	Sex	Mutation	GH peak (μg/L) to stimulants	IGF-1
[12]	3	M	2614fr/unknown (*SLC12A3*)	<8 (INS), <8 (ARG), <8 (CLN)	Not determined
	9	F	G186D/unknown (*SLC12A3*)	6 (CLN)	89ng/mL
[5]	3	M	Not determined	3.3 (L-DOPA), 7.3 (CLN)	0.26U/mL
	9	F	Not determined	9.2 (L-DOPA), 4.8 (CLN)	0.67U/mL
	19	F	Not determined	6.0 (CLN)	Not determined
[6]	7	M	Not determined	9.8 (INS + ARG)	Not determined
[11]	9	M	Not determined	2.1 (INS), 3.2 (CLN), 1.8 (L-DOPA)	55ng/mL
[13]	10	F	Not determined	7.5 (L-DOPA), 6.9 (CLN)	Normal
[14]	11	M	Not determined	10.8 (GRF), 7.0 (CLN)	0.43U/mL
[15]	11	M	Not determined	5 (INS), 1 (CLN), 13 (GRF)	292ng/mL
[4]	11	M	Not determined	11 (CLN), 3.1 (GLC)	0.74U/mL
[16]	13	M	Not determined	5.4 (INS), 5.4 (ARG), 12 (GLC-PPL)	0.19U/mL

Cases were categorized as Gitelman syndrome according to the authors' own judgment, even if they were described as Bartter syndrome in the original reports. *ARG* arginine, *CLN* clonidine, *L-DOPA* L-3,4-dihydroxyphenylalanine, *GH* growth hormone, *GLC* glucagon, *GRF* growth hormone releasing factor, *IGF-1* insulin-like growth factor 1, *INS* insulin, *PPL* propranolol.

Molecular diagnosis is a prerequisite for the detailed study of classic BS.

Tables 2 and 3 summarize cases of GHD reported to date classified as BS [2,3,7-10] and GS [4-6,11-16], respectively. Our patient's case is remarkable in that the diagnosis of classic BS was established molecularly. In addition, our patient's GH responses to pharmacological stimulants were most profoundly impaired among the hitherto reported cases. Although one may argue that hypokalemia may blunt the GH response and lead to false negative results, the excellent response to GH therapy made us suspicious for the presence of GHD. By adding our patient to the existing list of cases of GHD concomitant with BS, we believe that GHD should be regarded as a complication in classic BS.

Flyvbjerg *et al.* suggested that hypokalemia is a causative factor of GHD [17]. These authors stated that mice fed a low potassium diet showed growth retardation with low IGF-1 levels and attenuated GH response to GH-releasing factor (GRF). From this observation, hypokalemia seems to be one of the possible factors responsible for GHD in classic BS. This hypothesis is strengthened by the findings that GHD has also been reported in other diseases predisposing to hypokalemia, such as GS (Table 3) and the Bartter-like Dent disease [18]. In addition, this hypothesis can help to differentiate GHD (our patient in the present report) from non-GHD (his sister). Because large amounts of potassium could be administered via the gastric tube or tablets, a higher serum potassium level could be maintained in the sister, which may have prevented the development of GHD. Furthermore, the lack of association between GHD and antenatal BS, which is caused by mutations in either the *SLC12A1* (type I BS) or *KCNJ1* (type II BS) gene, can be explained by the observation that the correction of hypokalemia is generally easier in antenatal BS than in classic BS.

However, factors other than hypokalemia may be necessary for developing GHD. Patients with familial aldosteronism, rare genetic forms of primary aldosteronism, present with hypokalemia and some of them are refractory to medical therapy, yielding to long standing hypokalemia [19]. Regardless, GHD has not been reported to date in patients with familial aldosteronism. Thus, an aim of our future studies would be to determine the precise mechanism by which GHD develops in patients with classic BS.

Conclusions

In summary, we report our experience of profound GHD in a boy with mutations in the *CLCNKB* gene, and propose that GH status should be monitored while treating salt-losing tubulopathies including classic BS and GS.

Consent

Written informed consent was obtained from the patient's next-of-kin for publication of this case report and any accompanying images. A copy of the written consent is available for review by the Editor-in-Chief of this journal.

This study was approved by the Institutional Review Board of Kanagawa Children's Medical Center and followed the World Medical Association Declaration of Helsinki regarding ethical conduct of research involving human subjects.

Abbreviations

BS: Bartter syndrome; GH: Growth hormone; GHD: GH deficiency; GRF: GH-releasing factor; GS: Gitelman syndrome; IGF-1: Insulin-like growth factor 1.

Competing interests

The authors declare that they have no competing interests.

Authors' contributions

MA treated our patient from the beginning, performed the *CLCNKB* gene analysis and evaluated the GH status of our patient. MA also wrote the manuscript. TT and KM planned and performed the *CLCNKB* gene analysis. YA and KM critically reviewed and revised the manuscript. All authors read and approved the final manuscript.

Acknowledgements

We thank Ms Reiko Iwano, Department of Endocrinology and Metabolism, Kanagawa Children's Medical Center, Japan, for her excellent technical assistance.

Author details

[1]Department of Endocrinology and Metabolism, Kanagawa Children's Medical Center, Mutsukawa 2-138-4 Minami-ku, Yokohama 232-8555, Japan. [2]Department of Pediatrics, Hokkaido University School of Medicine, Sapporo 060-8635, Japan.

Received: 12 August 2013 Accepted: 28 October 2013
Published: 30 December 2013

References

1. Seyberth HW, Schlingmann KP: **Bartter- and Gitelman-like syndromes: salt-losing tubulopathies with loop or DCT defects.** *Pediatr Nephrol* 2011, **26**:1789–1802.
2. Bettinelli A, Borsa N, Bellantuono R, Syrèn ML, Calabrese R, Edefonti A, Komninos J, Santostefano M, Beccaria L, Pela I, Bianchetti MG, Tedeschi S: **Patients with biallelic mutations in the chloride channel gene CLCNKB: long-term management and outcome.** *Am J Kidney Dis* 2007, **49**:91–98.
3. Lefebvre J, Racadot A, Dequiedt P, Linquette M: **Électrolytes échangeables, glycorégulateur et hormone de croissance au cours d'un syndrome de Bartter [in French].** *Ann Endocrinol (Paris)* 1977, **38**:385–386.
4. Requeira O, Rao J, Baliga R: **Response to growth hormone in a child with Bartter's syndrome.** *Pediatr Nephrol* 1991, **5**:671–672.
5. Ruvalcaba RH, Martinez FE: **Case report: familial growth hormone deficiency associated with Bartter's syndrome.** *Am J Med Sci* 1992, **303**:411–414.
6. Boer LA, Zoppi G: **Bartter's syndrome with impairment of growth hormone secretion.** *Lancet* 1992, **340**:860.
7. Akil I, Ozen S, Kandiloglu AR, Ersoy B: **A patient with Bartter syndrome accompanying severe growth hormone deficiency and focal segmental glomerulosclerosis.** *Clin Exp Nephrol* 2010, **14**:278–282.
8. Buyukcelik M, Keskin M, Kilic BD, Kor Y, Balat A: **Bartter syndrome and growth hormone deficiency: three cases.** *Pediatr Nephrol* 2012, **27**:2145–2148.
9. Fukuyama S, Hiramatsu M, Akagi M, Higa M, Ohta T: **Novel mutations of the chloride channel Kb gene in two Japanese patients clinically**

diagnosed as Bartter syndrome with hypocalciuria. *J Clin Endocrinol Metab* 2004, **89**:5847–5850.
10. Nariai A, Yokoya S, Kato K: **A case of Bartter's syndrome with growth hormone deficiency [abstract].** *Clin Pediatr Endocrinol* 1993, **2**:165.
11. Ko CW, Koo JH: **Recombinant human growth hormone and Gitelman's syndrome.** *Am J Kidney Dis* 1999, **33**:778–781.
12. Bettinelli A, Rusconi R, Ciarmatori S, Righini V, Zammarchi E, Donati MA, Isimbaldi C, Bevilacqua M: **Gitelman disease associated with growth hormone deficiency, disturbances in vasopressin secretion and empty sella: a new hereditary renal tubular-pituitary syndrome?** *Pediatr Res* 1999, **46**:232–238.
13. Slyper AH: **Growth, growth hormone testing and response to growth hormone treatment in Gitelman syndrome.** *J Pediatr Endocrinol Metab* 2007, **20**:257–259.
14. Itagaki Y, Tagawa T, Fujii F, Tanabe Y, Sumi K, Nose O, Seino Y: **Bartter's syndrome with impairment of growth hormone secretion [abstract].** *Clin Pediatr Endocrinol* 1995, **4**:213.
15. Nariai A, Yokoya S, Tajima T: **Final height in two growth hormone-deficient patients with Bartter's syndrome treated with growth hormone in combination with luteinizing hormone-releasing hormone analog [abstract].** *Clin Pediatr Endocrinol* 2003, **12**:166.
16. Yokoyama T, Ohyanagi K: **A child case of Bartter syndrome with chronic renal failure treated by recombinant human hormones [abstract].** *Clin Pediatr Endocrinol* 1992, **1**:57.
17. Flyvbjerg A, Dørup I, Everts ME, Orskov H: **Evidence that potassium deficiency induces growth retardation through reduced circulating levels of growth hormone and insulin-like growth factor I.** *Metabolism* 1991, **40**:769–775.
18. Bogdanović R, Draaken M, Toromanović A, Dordević M, Stajić N, Ludwig M: **A novel CLCN5 mutation in a boy with Bartter-like syndrome and partial growth hormone deficiency.** *Pediatr Nephrol* 2010, **25**:2363–2368.
19. Mulatero P, Monticone S, Rainey WE, Veglio F, Williams TA: **Role of KCNJ5 in familial and sporadic primary aldosteronism.** *Nat Rev Endocrinol* 2013, **9**:104–112.

doi:10.1186/1752-1947-7-283
Cite this article as: Adachi *et al.*: Classic Bartter syndrome complicated with profound growth hormone deficiency: a case report. *Journal of Medical Case Reports* 2013 **7**:283.

Novel Insights from Clinical Practice

HORMONE RESEARCH IN PÆDIATRICS

Horm Res Paediatr 2013;80:119–128
DOI: 10.1159/000353763

Received: January 18, 2013
Accepted: June 6, 2013
Published online: August 21, 2013

Characteristic Testicular Histology Is Useful for the Identification of NR5A1 Gene Mutations in Prepubertal 46,XY Patients

Noriko Nishina-Uchida[a] Ryuji Fukuzawa[b] Chikahiko Numakura[d] Ayuko S. Suwanai[c] Tomonobu Hasegawa[c] Yukihiro Hasegawa[a]

[a]Department of Endocrinology and Metabolism and [b]Pathology and Clinical Laboratory, Tokyo Metropolitan Children's Medical Center, Tokyo, and [c]Department of Pediatrics, School of Medicine, Keio University, Tokyo, and [d]Department of Pediatrics, Faculty of Medicine, Yamagata University, Yamagata, Japan

Established Facts

- Leydig cells are not visible microscopically before puberty and their presence at this period is seen only in disorders of sexual development (DSD).
- The histological features of patients with *NR5A1* mutations have been described, but their clinical significance has not been fully established.

Novel Insights

- The key histological characteristics in the prepubertal testis of 46,XY patients with *NR5A1* mutations are hypoplastic seminiferous tubules and the emergence of Leydig cells with vacuolar cytoplasms.
- We propose that testicular histology is a useful marker for the identification of *NR5A1* mutations in 46,XY patients with DSD before puberty.

Key Words
Leydig cells · Steroidogenic factor-1 · Testicular histology · Steroidogenic acute regulatory protein

Abstract
Background: Individuals with *NR5A1* mutations encoding steroidogenic factor-1 (SF1) develop a phenotypically broad range of disorders of sexual development (DSD). Based on a literature review, we noted that hypoplastic seminiferous tubules and the emergence of Leydig cells with vacuolar cytoplasms are seen predominantly in the majority of individuals with *NR5A1* mutations. ***Aim:*** The aim of this study was to address whether the histopathological characteristics of the testis can be a biomarker for 46,XY individuals with *NR5A1* mutations. ***Design:*** In order to ascertain whether or not the histological features were the characteristics of *NR5A1* mutations, we screened the testicular histology of 242 patients

KARGER

E-Mail karger@karger.com
www.karger.com/hrp

1663–2818/13/0802–0119$38.00/0

Ryuji Fukuzawa, MD, PhD
Pathology and Clinical Laboratory
Tokyo Metropolitan Children's Medical Center
2-8-29 Musashidai, Fuchu, Tokyo 183-8561 (Japan)
E-Mail fukuzawa@1998.jukuin.keio.ac.jp

with 46,XY DSD and then subsequently assessed *NR5A1* mutations. ***Result:*** Of 242 patients with 46,XY DSD, 6 patients matched histological testicular features: a reduced number of thin seminiferous tubules and focal aggregations of Leydig cells that contained cytoplasmic lipid droplets. All 6 patients had *NR5A1* mutations. These histological features were distinct from those of other DSD. Thus, this unique testicular histology is useful for identifying *NR5A1* mutations in 46,XY patients with DSD before puberty.

Introduction

The development and maturation of Leydig cells are dynamic processes involving interactions between hormones and differentiation of the male reproduction system [1]. Three distinct populations of Leydig cells have been described during testis development [2]. The fetal Leydig cell population undergoes the greatest increase in number during the second trimester, and they eventually become hyperplasic because of high levels of androgen hormone secretion [1]. Androgen hormone secretion from Leydig cells decreases following the virilization of the external genitalia and differentiation of the Wolffian duct, and the Leydig cells undergo involution after birth [3]. The infantile Leydig cell population appears a few months after birth and disappears shortly thereafter until puberty, during a period called minipuberty [4]. The adult Leydig cell population arises at puberty and maintains androgen production throughout adult life [1, 5]. It is hypothesized that Leydig cells adopt a fibroblastic phenotype and disappear from the postnatal time to puberty. Nevertheless, it is well established that Leydig cells are not histologically visible in the prepubertal testis.

Steroidogenic factor-1 (SF1; AD4BP; OMIM 184757), encoded by the *NR5A1* gene, is a nuclear receptor that regulates adrenal and reproductive development and function [6, 7]. Its role in mammalian development has been clarified using homozygous *nr5a1* knockout mice, which show a complete failure of adrenal and gonadal development, XY sex reversal, persistence of Müllerian structures in males, and impaired function of pituitary gonadotropes [8]. On immunohistochemical examination, expression of SF1 is initially observed in the sexually undifferentiated gonads of human embryos, then in the interstitial cells (the precursor of the Leydig cell) of the early testis, and then confined to Sertoli cells and Leydig cells later in testicular development [9]. These observations indicate that SF1 plays an important role in the differentiation, development, and function of Leydig cells.

The first human *NR5A1* mutation was found in a patient with 46,XY who had XY sex reversal and adrenal failure [10]. Since then, over 50 patients carrying *NR5A1* mutations have been reported [11–13]. The patients with *NR5A1* mutations had a broad range of external genitalia phenotypes that included normal-appearing female, ambiguous genitalia, hypospadias, undescended testes, anorchia, isolated micropenis, and normal male external genitalia with infertility [11–13]. The histological features of those patients have been described [10, 12, 14–21], but their clinical significance has not been fully established. We reviewed the literature and noted that some histological features were distinctive and were commonly seen in many patients with *NR5A1* mutations. Therefore, we examined our cohort to ascertain if the histological characteristics could be a surrogate maker for *NR5A1* mutations.

Patients and Methods

Literature Search

We reviewed the literature to search for clinical and histopathological features of patients with *NR5A1* mutations [10–12, 14–21]. Based on this review, we considered that there were three major histological types as follows (table 1): (1) streak gonads consisting of poorly formed seminiferous tubules in the connective tissue, (2) absence of the testicular tissue, and (3) testes composed of hypoplastic seminiferous tubules and/or the emergence of Leydig cells with occasional vacuolar cytoplasms. Both histological changes should be simultaneously found in a testis; however, descriptions concerning the presence of Leydig cells and the appearance of seminiferous tubules were occasionally incomplete. We hypothesized that hypoplastic seminiferous tubules and/or the presence of Leydig cells with vacuolar cytoplasms are the key pathological features of prepubertal 46,XY female patients with *NR5A1* mutations since either or both of these histological features are frequently described (table 1). We next investigated the relationship between these testicular histological features and the clinical subtype with *NR5A1* mutations. In order to determine the frequency of the histological characteristics in each clinical subtype, the patients with *NR5A1* mutations were classified as described by Achermann's group [11] with some modifications: type 1 = the typical 46,XY DSD phenotype characterized by ambiguous genitalia or clitorimegaly and absent or rudimentary Müllerian structures with undescended testes; type 2 = the severe 46,XY DSD phenotype represented by female external genitalia, a normal vagina, a normal uterus, and streak gonads; type 3 = hypospadias with small inguinal testes; type 4 = microphallus with or without bilateral anorchia, and type 5 = phenotypically normal men with nonobstructive male infertility (excluded from this study). In the current study, type 2 was defined as when the exter-

Table 1. Summary of previously published histological features of testes with *NR5A1* mutations

Patient No.	Age at gonadectomy	Seminiferous tubules	Germ cells	Leydig cells	Müllerian duct	*NR5A1* mutation	Ref.
1	4 months	abundant	many	ND	absent	V15M	[14]
2	4 months	decreased	present	ND	remnant	G91S	[14]
3	6 months	normal	normal	present	ND	c.536delC	[15]
4	6 months	normal	normal	ND	ND	c.536delC	[15]
5	7 months	decreased	sparse	vacuolated intersititial cell	remnant	M78I	[14]
6	15 months	immature	decreased	ND	absent	C16X	[16]
7	17 months	ND	decreased	marked	absent	R84C	[17]
8	18 months	ND	ND	hyperplasia	ND	W279X/G3314_3317delTCTC	[18]
9	2 years	ND	absent	aggregated Leydig cells	ND	Q206TfsX20	[12]
10	2 years	ND	absent	foamy Leydig cells	ND	L231_233dup	[12]
11	3.5 years	ND	ND	vacuolated Leydig cells	ND	H24T	[12]
12	4 years	ND	few	few	absent	C33S	[19]
13	4 years	ND	absent	few	absent	c.389delC	[12]
14	10 years	immature	ND	ND	present	G35E	[10]
15	10 months	immature	a few	absent	ND	R313H	[20]
16	6 years	atrophic	few	absent	ND	L437Q	[14]
17	4 years	atrophic	ND	ND	ND	V355M	[21]

Patient 14 was diagnosed as having streak gonads. In patient 17, the second biopsy at the age of 13 years showed an absence of testicular tissue. ND = Not described.

nal genitalia appeared to be complete female because information on the gonadal histology and the persistence of the Müllerian duct derivative was not always available. Patients with microphallus without anorchia were included in type 4. Type 5 was excluded because the patients in this category are normal-appearing males. Since Leydig cells are invisible until puberty and the presence of Leydig cells in prepuberty is a characteristic feature of *NR5A1* mutations, patients receiving gonadectomy at an age of 10 years or less were selected.

Patients and NR5A1 Mutation Analysis

In order to test whether or not the histological features proposed above could indeed predict the presence of *NR5A1* mutations, we screened for these features in 253 testes from 242 patients under 10 years of age with a 46,XY karyotype and abnormal sexual development who underwent gonadectomy or biopsy. These 242 patients were composed of 222 with unilateral or bilateral undescended testes, 5 with hypospadias with undescended testes, and 15 with ambiguous genitalia or complete female. To test whether other prepubertal patients with DSD lack the testicular histological features similar to patients with *NR5A1* mutations, we also histologically reviewed testes from patients with mixed gonadal dysgenesis (17 cases), androgen insufficiency (3 cases), Denys-Drash and Fraser syndromes (6 cases), and true hermaphroditism (4 cases) whose diagnoses were confirmed by cytogenetic or gene mutational analyses. Sequencing for *NR5A1* was performed on DNA from blood samples as previously described [22].

Written informed consent was obtained from the parents for the biochemical and molecular studies, which were approved by the ethical committee of Tokyo Metropolitan Children's Medical Center.

Pathological Examination

Testes that had the distinctive histological features were further examined to support the histological characteristics. Oil red O stain, immunohistochemistry, and electron microscopy were performed according to standard procedures. The following primary antibodies were used: SF1 (PMX, N1665, dilution 1:100) for the identification of Leydig cells and Sertoli cells, and WT1 (Nichirei, 6F-H2, diluted) and/or SOX9 (abcam, ab76997, dilution 1:100) for Sertoli cells. The size and number of the lumens of seminiferous tubules were quantified by morphometric analysis: the mean tubular diameter of each lumen and the number of tubules per unit area (0.64 mm^2) were measured using a digital image analyzer (WinRoof, Mitani Corp., Japan). After discrimination of Sertoli cells from spermatogonia by WT1 and/or SOX9 immunostaining, the number of spermatogonia per 10 tubular cross-sections and Sertoli cell number per tubular section were counted using the digital image analyzer. The resulting data were compared with previously published studies [23].

Results

Literature Review

The proportion of 46,XY DSD subtypes in 48 patients is shown in table 2, of which gonadal histology with the age of 10 years and less was available for 17 patients (tables 1, 3). Sixteen of 17 patients (94.2%) had hypoplastic seminiferous tubules and/or Leydig cells (table 3). Of

Table 2. The proportion of subtypes of patients with *NR5A1* mutations

Subtype	1	2	3	4	Summary
Number	30	7	9	2	48
Percent	62.5	14.6	18.7	4.2	100

Table 3. Relationship between histological type and clinical subtype in 46XY DSD with *NR5A1* mutations

	Type 1	Type 2	Type 3	Type 4	Summary
HST and/or Leydig cells	13[a]		2[b]	1	16
Streak		1			1
Anorchia					0

HST = Hypoplastic seminiferous tubules; Streak = streak gonads. All patients were under 10 years of age at gonadectomy.
[a] 1 case had no Leydig cells. [b] Both cases lacked Leydig cells.

these 16 cases, 13 (81.2%) belonged to the most common subtype (type 1; tables 2, 3), and the other 3 cases were types 3 and 4. Although there was a strong relationship between the proposed histological features and type 1 clinical phenotype, the histological features were also observed in other clinical subtypes, indicating that these histological features are common to patients with *NR5A1* mutations.

Identification of NR5A1 Mutations Based on Characteristic Histological Features

To test whether or not the two characteristic histological features could identify *NR5A1* mutations, we screened the histology of 253 testes from 242 patients with 46,XY. Among 253 testes, 6 patients had the matched histological characteristics (fig. 1a–h). As expected, all 6 patients had *NR5A1* mutations, all of which were novel mutations. Case 4 was recently reported [24]. The clinical, laboratory, and *NR5A1* mutation data for these 6 patients are summarized in table 4. Four of 6 cases fell into the category of the typical clinical phenotype (type 1), while 1 case had hypospadias with undescended testes (type 3). Although case 5 had completely female external genitalia, the testicular histology did not show streak gonads (fig. 1g, n). Thus, this patient might be classifiable as type 1 rather than type 2. The pathological significance of the identified mutations was confirmed by examining functional assays (unpubl. data). Remarkably, 3 patients (1–3 years of age) with undescended testes who received hCG load tests were included in this cohort, and none of them had *NR5A1* mutations. Thus, these cases eliminated the possibility that the hCG load test influenced the emergence of Leydig cells, and further supported the relationship between *NR5A1* mutations and the presence of Leydig cells. The characteristic histological features described in this study were not found in mixed gonadal dysgenesis, androgen insufficiency, Denys-Drash and Fraser syndromes, or true hermaphroditism (data not shown).

Detailed Pathological Evaluation for the Testes with NR5A1 Mutations

The pathological changes of the seminiferous tubules that underlie testicular hypoplasia and the emergence of Leydig cells with lipid accumulation were further examined by morphometric, immunohistochemical, and ultrastructural analyses. On gross examination, testicular hypoplasia was evident because the testicular parenchymas looked smaller as compared to the patients' epididymides (fig. 1a). Histologically, the testicular parenchyma consisted of a decreased number of seminiferous tubules. The seminiferous tubules were thin in younger patients (fig. 1b); however, the lumens of the seminiferous tubules tended to dilatate with age (fig. 1i, l), as is generally seen in testes with atrophy. The number of spermatogonia was decreased (fig. 1c, d, f–h, k–p). Sertoli cells had round or oval-shaped pyknotic nuclei and inconspicuous cytoplasms (fig. 1c, d, f–h). SF1, WT1, and SOX9 were expressed in the nuclei of the Sertoli cells (fig. 1k–p). The interstitium was often edematous, in which seminiferous tubules occasionally lacked back-to-back structures (fig. 1b). Case 3 was the oldest patient in our cohort whose testes were barely identifiable on microscopic examination. The seminiferous tubules were greatly reduced in number and showed atrophy and dilatation, suggesting that in addition to congenital hypoplasia, atrophic changes occurred secondarily. The second characteristic histological feature was the presence of focal aggregations of interstitial cells with foamy cytoplasms (fig. 1c–h), indicating the Leydig cells had intracytoplasmic accumulation of lipids. Nuclear immunostaining for SF1 confirmed that these interstitial cells were Leydig cells (fig. 1k–n). Lipid deposition in the cytoplasm was confirmed by oil red O staining (fig. 1i) and electron microscopic examination (fig. 1j). Müllerian duct remnants were not found in these 6 patients. The reduced size and number of sem-

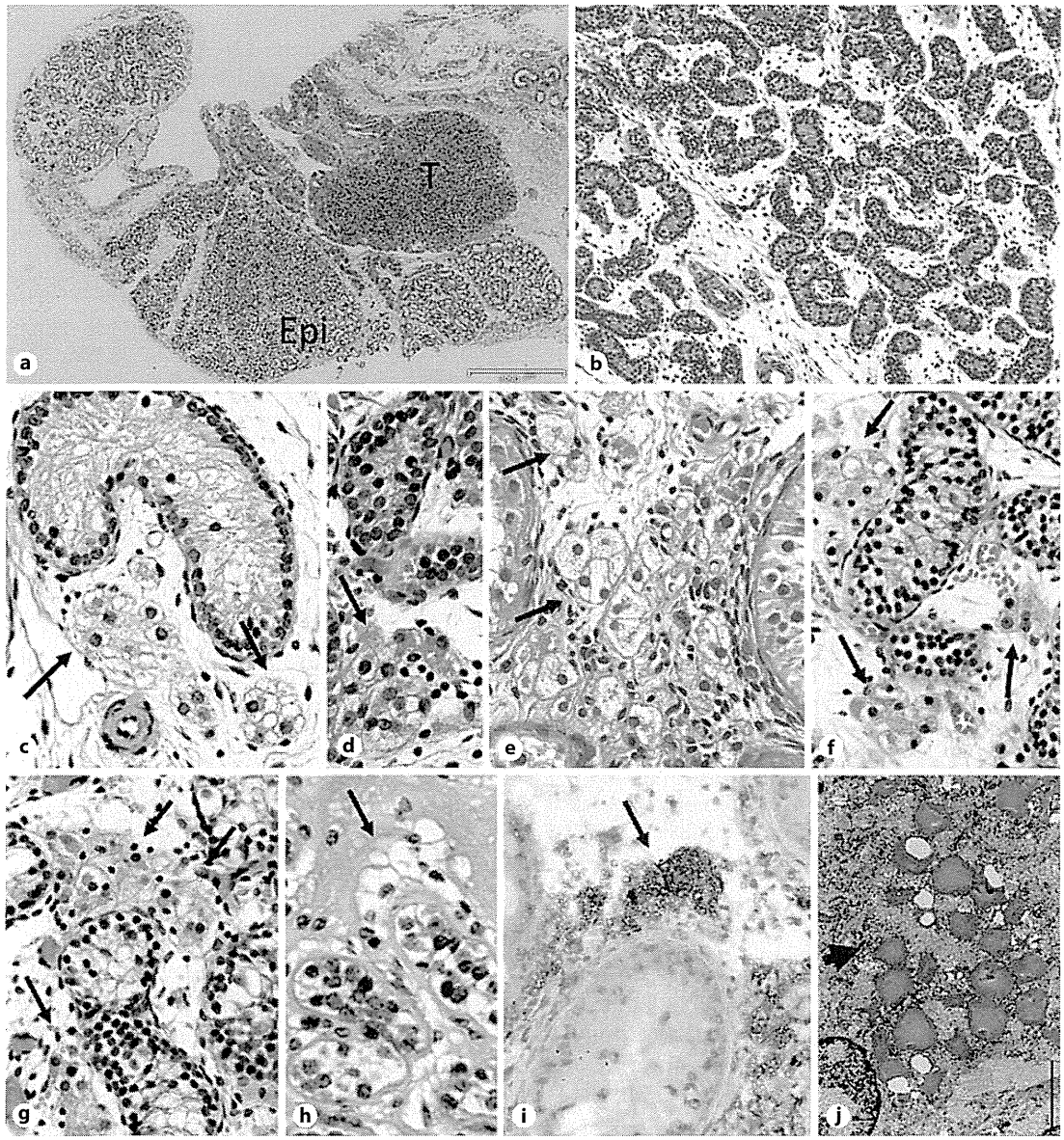

Color version available online

Fig. 1. Pathological features of testes with *NR5A1* mutations. **a** Scanned image of a representative longitudinally bisected testis (case 1) showing a smaller testicular parenchyma (T) compared to the attached epididymis (Epi). **b** Microphotograph of a testicular parenchyma (case 2) revealing a decreased number of thin seminiferous tubules in the edematous loose connective tissue. High-power view of aggregated foamy Leydig cells (**c**, case 1; **d**, case 2; **e**, case 3; **f**, case 4; **g**, case 5; **h**, case 6; indicated by arrows). Note that spermatogonia are rarely seen in the seminiferous tubules. **i** Oil red O staining proving the accumulation of lipid droplets indicated by arrows (case 3). **j** Electron microscopy of Leydig cells (case 3) containing lipid droplets (high electron density deposits indicated by arrow heads).

iniferous tubules with a decreased number of spermatogonia underlying testicular hypoplasia were confirmed by the morphometric analysis (fig. 2a–c; table 5a, b), while the number of Sertoli cells was not significantly decreased.

Discussion

We confirmed the testicular histology associated with *NR5A1* mutations: hypoplastic testes are attributable to the reduced size and number of seminiferous tubules,

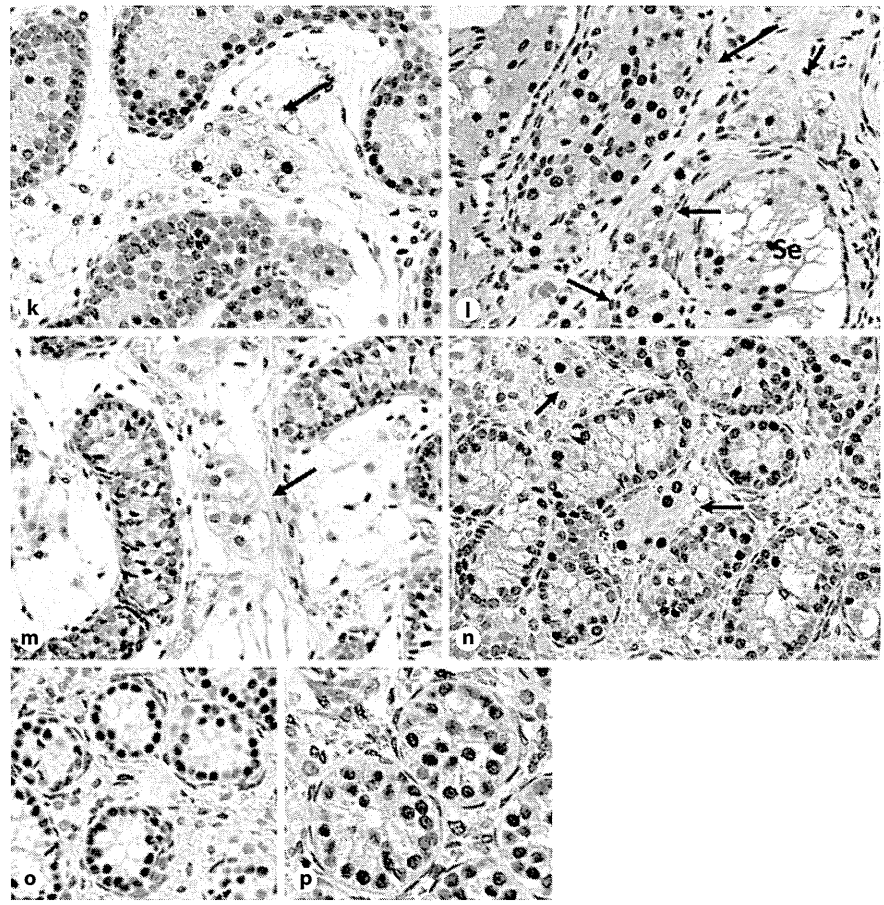

Color version available online

Fig. 1. Pathological features of testes with *NR5A1* mutations. Immunohistochemistry for SF1 localizing in the nucleus confirming the emergence of Leydig cells indicated by arrows (**k**, case 1; **l**, case 3; **m**, case 4; **n**, case 5). SF1 is also expressed in Sertoli cells in the seminiferous tubules (Se). Sertoli cells have round or oval shaped nuclei expressing WT1 (**o**, case 5) and SOX9 (**p**, case 5) and inconspicuous cytoplasms. Original magnification ×200 (**b**), ×600 (**c–i**, **k–o**), ×400 (**p**).

which consist of round or oval-shaped Sertoli cells and few spermatogonia. Leydig cells are present with cytoplasmic lipid accumulations. We found that the histology is distinct from that of other DSD. The literature search demonstrated that these histological features are observed in the majority of patients with *NR5A1* mutations regardless of clinical subtype. Since the clinical features of types 1 and 2 46,XY DSD overlap considerably, type 2 therefore includes a number of patients who have the same histological features, such as we observed in case 5. It is thought that the pure form of patients with type 2 46,XY DSD essentially have streak gonads, but such patients are rare. Type 3 is the second most common subtype, whose testicular histology is rarely available because histopathological examination is seldom performed on undescended testes. We assume that type 3 patients also have the characteristic histological features because case 6 had identical histological features. An absence of Leydig cells was noted in 2 cases (table 1, patient Nos. 15 and 16). However, we could not confirm the absence of Leydig cells in these patients because the histologic evaluation was not performed on orchidectomy, but on biopsy samples which occasionally contain too little testicular parenchyma to reliably have any potential Leydig cells. Type 4 is also a rare subtype. Because anorchia (absence of the testicular tissue) results from secondary regressive changes, the testes originally might have also had the same histological characteristics. Type 5 was excluded from this study because the patients in this category are normal-appearing males. All types taken together, the characteristic histology is expected to be helpful for the identification of *NR5A1* mutations, but its utility would be limited for prepubertal patients with DSD.

It is conceivable that pathological changes in the testis with a *NR5A1* mutation primarily occur in Leydig cells and Sertoli cells because expression of SF1 is confined to these two cell types during testicular development. Dys-

Table 4. Clinical features and laboratory data of 6 patients with *NR5A1* mutations

Patient No.	Subtype	Mutation	Karyotype/ assigned gender	External genitalia	Müllerian duct	Age at gonadectomy	LH mIU/ml	FSH mIU/ml	Testosterone ng/ml[a]	Adrenal function
1	1	C13R	46,XY female	clitorimegaly	absent	1.6 years	basal ND peak 0.1	basal ND peak 6.5	basal <0.05 peak 0.20 (3 months)	normal
2	1	c.227_260del34	46,XY female	clitorimegaly	absent	6 months	basal 0.8 peak 7.9	basal 4.7 peak 4.8	basal 0.06 peak 0.61 (2 months)	normal
3	1	G26fsX5	46,XY female	clitorimegaly	absent	9.4 years	basal 2 peak 42.5	basal 37.6 peak 3.1	basal 0.17 peak 0.74 (9.4 years)	normal
4	1	D257TfsX39	46,XY female	clitorimegaly	absent	1.1 years	basal ND peak 3.2	basal ND peak 7.2	basal 0.92 peak 2.11 (1.1 years)	normal
5	2	P205fsX90	46,XY female	complete female	absent	4.3 years	basal 0.1 peak 10	basal 0.8 peak 7.9	basal 0.11 peak 1.33 (2.8 years)	normal
6	3	c.870+3_6delGAGT	46,XY male	hypospadia, bilateral cryptorchidism	absent	4 years	ND	ND	basal 0.17 peak 0.94 (9.4 years)	normal

[a] hCG stimulation (3,000 IU/m^2 intramuscularly daily for 3 days). ND = Not done.

function of Leydig cells is thought to be the main pathogenetic cause that explains the varying degrees of impaired sexual development of children with *NR5A1* mutations. Leydig cells are normally histologically invisible until puberty [3]; nevertheless, in patients with *NR5A1* mutations, Leydig cells are present with lipid accumulation. It can be speculated that accumulations of lipids in the Leydig cells disturb their ability to undergo the morphological change into a fibroblast-like phenotype, as normally occurs between the postnatal periods and puberty [3]. Therefore, the Leydig cells might be persistently identifiable. Alternatively, overstimulation of Leydig cells by human chorionic gonadotropin from syncytiotrophoblasts might cause emergence, hyperplasia, and persistence of Leydig cells beyond fetal stages. In a recent immunohistochemical study, Cools et al. [25] detected granular patterns of the SF1 protein in the cytoplasms of Leydig cells of 2 patients with *NR5A1* mutations, as well as those of adult Leydig cells. However, none of our 6 cases with *NR5A1* mutations showed a cytoplasmic granular SF1 staining pattern in Leydig cells, despite our use of the same SF1 antibody. The different SF1 immunostaining patterns between the two studies might be age related, as 2 patients in their study were 12 and 13 years of age, while all of our patients were under 10 years of age. On the other hand, Sertoli cells were thought to be functionally normal during the fetal period because of the absence of Müllerian structures and expression of WT1, SOX9, and SF1 in Sertoli cells without significant reduction in their number. Therefore, the morphological changes might have occurred secondarily.

Patients with *NR5A1* and steroidogenic acute regulatory protein *(StAR)* mutations share similar testicular histological features characterized by the presence of Leydig cells with lipid accumulation [26]. It is known that SF1 binds the *StAR* promoter and regulates its transcriptional activity leading to sex differentiation [27]. *NR5A1* mutations might cause accumulation of steroids in the Leydig cells through the same mechanism caused by *StAR* mutations. However, the mechanism remains to be elucidated. Interestingly, the histopathological features of the testes caused by the two mutations are largely different except for the presence of foamy Leydig cells. In *StAR* deficiency, seminiferous tubules develop nor-

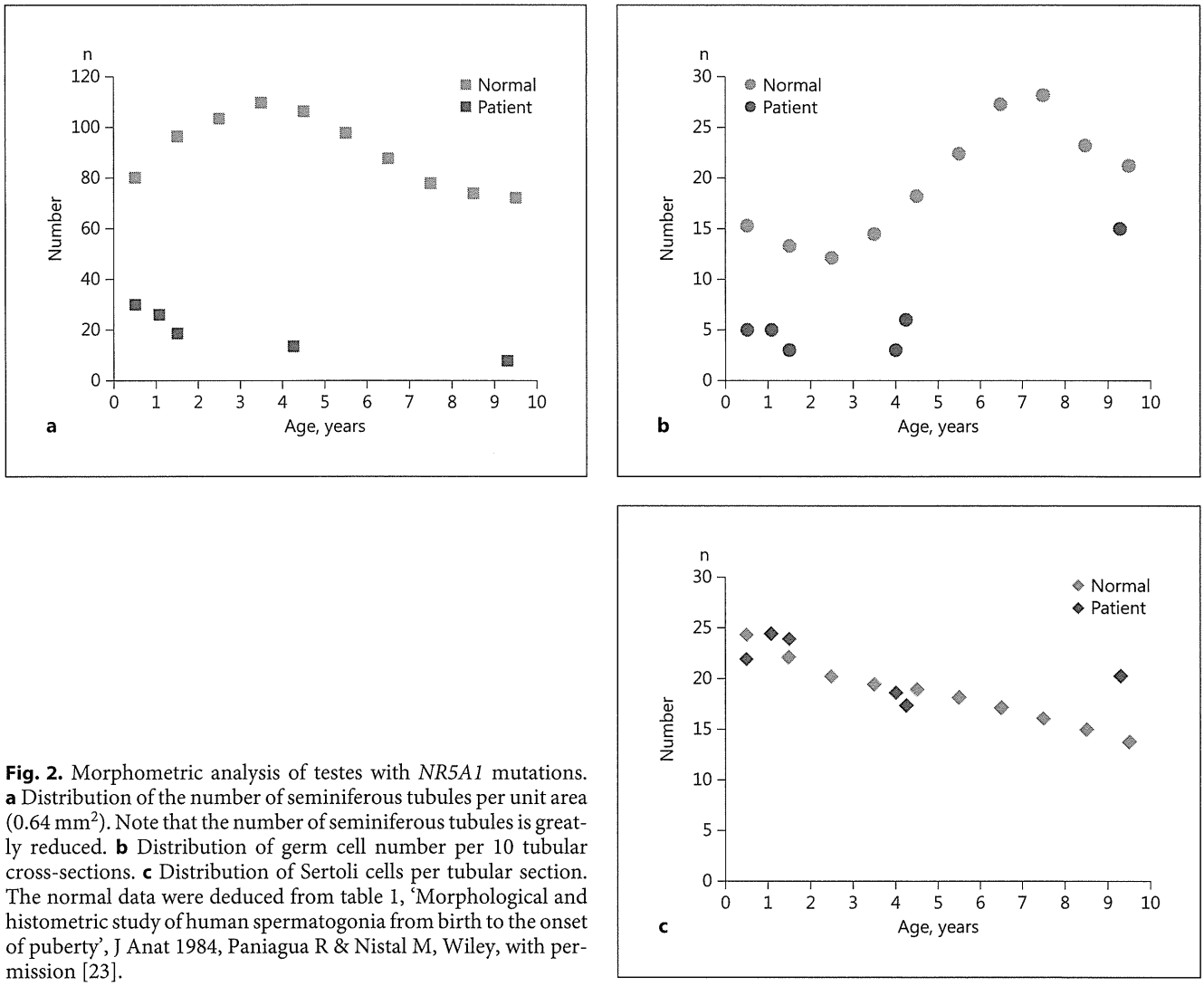

Color version available online

Fig. 2. Morphometric analysis of testes with *NR5A1* mutations. **a** Distribution of the number of seminiferous tubules per unit area (0.64 mm^2). Note that the number of seminiferous tubules is greatly reduced. **b** Distribution of germ cell number per 10 tubular cross-sections. **c** Distribution of Sertoli cells per tubular section. The normal data were deduced from table 1, 'Morphological and histometric study of human spermatogonia from birth to the onset of puberty', J Anat 1984, Paniagua R & Nistal M, Wiley, with permission [23].

mally, and germ cells in the seminiferous tubules are usually intact [28]. Thus, it is suggested that cells with *StAR* deficiency retain some capacity for androgen biosynthesis. In addition, the Sertoli cells can properly produce anti-Müllerian hormone, as the Müllerian duct completely regresses as usual. The size of the seminiferous tubules with *NR5A1* mutations is hypoplastic, while that of the testis with *StAR* mutations is normal at birth and becomes larger with more prominent lipid accumulation in Leydig cells with age [28]. Since *NR5A1* acts early in testicular development [9], it may regulate the size and the number of the seminiferous tubules, leading to a decreased number of Sertoli cells and germ cells. Leydig cells with *NR5A1* mutations do not become hypertrophic as compared to those with *StAR* mutations. This difference indicates that *StAR* might not be strictly regulated by SF1 in vivo.

Leydig cells can also sometimes be seen in other 46,XY DSD patients before puberty [29]. These include androgen dysfunction disorders (androgen insensitivity syndrome, 5α-reductase type II mutations) and mixed gonadal dysgenesis. As the testicular histology of androgen dysfunction disorders is similar to that of the cryptorchid testis, it might resemble that of *NR5A1* mutations [29]. However, neither congenital testicular hypoplasia nor foamy Leydig cells would be observed. The testicular histology of mixed gonadal dysgenesis is occasionally composed of abnormal architecture including areas of imma-

Table 5. Mean tubular diameter, number of tubules per unit area, and number of spermatogonia per 10 tubular cross-sections of prepubertal testes with normal (**a**) and *NR5A1* mutations (**b**)

a Normal control

	0–1 year	1–2 years	2–3 years	3–4 years	4–5 years	5–6 years	6–7 years	7–8 years	8–9 years	9–10 years
Mean tubular diameter, μm	84.1±2.0	77.4±2.1	74.5±1.9	72.1±1.8	70.0±1.3	71.9±1.5	74.4±1.5	77.5±1.4	80.2±1.7	83.9±1.9
Number of tubules per unit area (0.64 mm^2)	80.1±1.8	96.4±2.2	103.5±2.7	109.8±2.6	106.2±2.5	97.7±2.1	87.5±1.9	77.8±1.8	74.0±1.3	72.2±1.4
Number of spermatogonia per 10 tubular cross-sections	15.3±1.2	13.3±1.3	12.1±1.0	14.5±1.3	18.2±1.6	22.4±1.9	27.3±2.5	28.2±2.6	23.2±2.2	21.1±1.8
Sertoli cell number per tubular cross-section	24.4±0.3	22.2±0.3	20.3±0.3	19.5±0.3	19.0±0.3	18.2±0.3	17.2±0.3	16.1±0.2	15.0±0.2	13.8±0.2

Data are expressed as means ± SD per age group. Confidence limits are 99%. Data are deduced from table 1, 'Morphological and histometric study of human spermatogonia from birth to the onset of puberty', J Anat 1984, Paniagua R & Nistal M, Wiley, with permission [23].

b Patients with *NR5A1* mutations

	Patient 1 1.6 years	Patient 2 (lt) 6 months	Patient 3 (rt) 9.4 years	Patient 4 1.1 years	Patient 5 (rt) 4.3 years	Patient 6 (rt) 4 years
Mean tubular diameter, μm	22.5±0.7	30±3	8±1	26.1±1	13.7±3.4	52.5±0.7
Number of tubules per unit area (0.64 mm^2)	60.8±8.3	46.9±3.0	153.9±29.7	57.1±4.8	88.9±11.2	39.9±5.7
Number of spermatogonia per 10 tubular cross-sections	3	5	15	5	1	3
Sertoli cell number per tubular cross-section	24±2.6	22±2.5	20.3±5.1	24.5±1.7	17.4±2.0	18.7±4.0

Number of tubules per unit area, number of spermatogonia per 10 tubular cross-sections, and Sertoli cell number per tubular cross-section are plotted in fig. 2a–c, respectively.

ture primary sex cords indeterminate between female and male structures [29]. Thus, the histologic features are totally different from those of *NR5A1* mutations. In this study, we have ascertained that the other DSD patients with mixed gonadal dysgenesis, androgen insufficiency, Denys-Drash and Fraser syndromes, and true hermaphroditism lacked the testicular histological features similar to patients with *NR5A1* mutations.

In conclusion, we propose that testicular histological characteristics are a useful biomarker for the identification of *NR5A1* mutations in prepubertal 46,XY patients with DSD.

References

1 Svechnikov K, Landreh L, Weisser J, Izzo G, Colon E, Svechnikova I, Soder O: Origin, development and regulation of human Leydig cells. Horm Res Paediatr 2010;73:93–101.
2 Pelliniemi LJ, Niemi M: Fine structure of the human foetal testis. I. The interstitial tissue. Z Zellforsch Mikrosk Anat 1969;99:507–522.
3 Gilbert-Barness E, Gunasekaran S, Scully R: 4th; in Gilbert-Barness E (ed): Potter's Pathology of the Fetus and Infant, ed 1. St Louis, Mosby, 1997, p 1204.
4 Forest MG, Sizonenko PC, Cathiard AM, Bertrand J: Hypophyso-gonadal function in humans during the first year of life. 1. Evidence for testicular activity in early infancy. J Clin Invest 1974;53:819–828.
5 Griswold SL, Behringer RR: Fetal Leydig cell origin and development. Sex Dev 2009;3:1–15.
6 Woodson KG, Crawford PA, Sadovsky Y, Milbrandt J: Characterization of the promoter of SF-1, an orphan nuclear receptor required for adrenal and gonadal development. Mol Endocrinol 1997;11:117–126.
7 Lin L, Achermann JC: Steroidogenic factor-1 (SF-1, Ad4BP, NR5A1) and disorders of testis development. Sex Dev 2008;2:200–209.
8 Parker KL, Schimmer BP: Steroidogenic factor 1: A key determinant of endocrine development and function. Endocr Rev 1997;18:361–377.
9 de Santa Barbara P, Moniot B, Poulat F, Berta P: Expression and subcellular localization of SF-1, SOX9, WT1, and AMH proteins during early human testicular development. Dev Dyn 2000;217:293–298.

10 Achermann JC, Ito M, Hindmarsh PC, Jameson JL: A mutation in the gene encoding steroidogenic factor-1 causes XY sex reversal and adrenal failure in humans. Nat Genet 1999;22:125–126.
11 Ferraz-de-Souza B, Lin L, Achermann JC: Steroidogenic factor-1 (SF-1, NR5A1) and human disease. Mol Cell Endocrinol 2011;336: 198–205.
12 Camats N, Pandey AV, Fernandez-Cancio M, Andaluz P, Janner M, Toran N, Moreno F, Bereket A, Akcay T, Garcia-Garcia E, Munoz MT, Gracia R, Nistal M, Castano L, Mullis PE, Carrascosa A, Audi L, Fluck CE: Ten novel mutations in the NR5A1 gene cause disordered sex development in 46,XY and ovarian insufficiency in 46,XX individuals. J Clin Endocrinol Metab 2012;97:E1294–E1306.
13 Bashamboo A, Ferraz-de-Souza B, Lourenco D, Lin L, Sebire NJ, Montjean D, Bignon-Topalovic J, Mandelbaum J, Siffroi JP, Christin-Maitre S, Radhakrishna U, Rouba H, Ravel C, Seeler J, Achermann JC, McElreavey K: Human male infertility associated with mutations in NR5A1 encoding steroidogenic factor 1. Am J Hum Genet 2010; 87:505–512.
14 Lin L, Philibert P, Ferraz-de-Souza B, Kelberman D, Homfray T, Albanese A, Molini V, Sebire NJ, Einaudi S, Conway GS, Hughes IA, Jameson JL, Sultan C, Dattani MT, Achermann JC: Heterozygous missense mutations in steroidogenic factor 1 (SF1/Ad4BP, NR5A1) are associated with 46,XY disorders of sex development with normal adrenal function. J Clin Endocrinol Metab 2007;92: 991–999.
15 Coutant R, Mallet D, Lahlou N, Bouhours-Nouet N, Guichet A, Coupris L, Croue A, Morel Y: Heterozygous mutation of steroidogenic factor-1 in 46,XY subjects may mimic partial androgen insensitivity syndrome. J Clin Endocrinol Metab 2007;92:2868–2873.
16 Mallet D, Bretones P, Michel-Calemard L, Dijoud F, David M, Morel Y: Gonadal dysgenesis without adrenal insufficiency in a 46,XY patient heterozygous for the nonsense C16X mutation: a case of SF1 haploinsufficiency. J Clin Endocrinol Metab 2004;89:4829–4832.
17 Reuter AL, Goji K, Bingham NC, Matsuo M, Parker KL: A novel mutation in the accessory DNA-binding domain of human steroidogenic factor 1 causes XY gonadal dysgenesis without adrenal insufficiency. Eur J Endocrinol 2007;157:233–238.
18 Warman DM, Costanzo M, Marino R, Berensztein E, Galeano J, Ramirez PC, Saraco N, Baquedano MS, Ciaccio M, Guercio G, Chaler E, Maceiras M, Lazzatti JM, Bailez M, Rivarola MA, Belgorosky A: Three new SF-1 (NR5A1) gene mutations in two unrelated families with multiple affected members: within-family variability in 46,XY subjects and low ovarian reserve in fertile 46,XX subjects. Horm Res Paediatr 2011;75:70–77.
19 Kohler B, Lin L, Ferraz-de-Souza B, Wieacker P, Heidemann P, Schroder V, Biebermann H, Schnabel D, Gruters A, Achermann JC: Five novel mutations in steroidogenic factor 1 (SF1, NR5A1) in 46,XY patients with severe underandrogenization but without adrenal insufficiency. Hum Mutat 2008;29:59–64.
20 Ciaccio M, Costanzo M, Guercio G, De Dona V, Marino R, Ramirez PC, Galeano J, Warman DM, Berensztein E, Saraco N, Baquedano MS, Chaler E, Maceiras M, Lazzatti JM, Rivarola MA, Belgorosky A: Preserved fertility in a patient with a 46,XY disorder of sex development due to a new heterozygous mutation in the NR5A1/SF-1 gene: evidence of 46,XY and 46,XX gonadal dysgenesis phenotype variability in multiple members of an affected kindred. Horm Res Paediatr 2012;78:119–126.
21 Philibert P, Zenaty D, Lin L, Soskin S, Audran F, Leger J, Achermann JC, Sultan C: Mutational analysis of steroidogenic factor 1 (NR5a1) in 24 boys with bilateral anorchia: a French collaborative study. Hum Reprod 2007;22:3255–3261.
22 Wong M, Ramayya MS, Chrousos GP, Driggers PH, Parker KL: Cloning and sequence analysis of the human gene encoding steroidogenic factor 1. J Mol Endocrinol 1996; 17:139–147.
23 Paniagua R, Nistal M: Morphological and histometric study of human spermatogonia from birth to the onset of puberty. J Anat 1984;139: 535–552.
24 Suwanai AS, Ishii T, Haruna H, Yamataka A, Narumi S, Fukuzawa R, Ogata T, Hasegawa T: A report of two novel NR5A1 mutation families: possible clinical phenotype of psychiatric symptoms of anxiety and/or depression. Clin Endocrinol (Oxf) 2013;78:957–965.
25 Cools M, Hoebeke P, Wolffenbuttel KP, Stoop H, Hersmus R, Barbaro M, Wedell A, Bruggenwirth H, Looijenga LH, Drop SL: Pubertal androgenization and gonadal histology in two 46,XY adolescents with NR5A1 mutations and predominantly female phenotype at birth. Eur J Endocrinol 2012;166:341–349.
26 Bose HS, Sugawara T, Strauss JF 3rd, Miller WL: The pathophysiology and genetics of congenital lipoid adrenal hyperplasia. N Engl J Med 1996;335:1870–1878.
27 Sugawara T, Lin D, Holt JA, Martin KO, Javitt NB, Miller WL, Strauss JF 3rd: Structure of the human steroidogenic acute regulatory protein (StAR) gene: StAR stimulates mitochondrial cholesterol 27-hydroxylase activity. Biochemistry 1995;34:12506–12512.
28 Hasegawa T, Zhao L, Caron KM, Majdic G, Suzuki T, Shizawa S, Sasano H, Parker KL: Developmental roles of the steroidogenic acute regulatory protein (StAR) as revealed by StAR knockout mice. Mol Endocrinol 2000; 14:1462–1471.
29 Al-Ahmadie HA: The male reproductive system, including intersex disorders; in Stocker JT, Dehner LP, Husain AN (eds): Stocker and Dehner's Pediatric Pathology, ed 3. Philadelphia, Lippincott Williams & Wilkins, 2011, pp 865–896.

PEDIATRICS INTERNATIONAL Official Journal of the Japan Pediatric Society

Pediatrics International (2013) **55**, e103–e106 doi: 10.1111/ped.12098

Patient Report

Case of an infant with hepatic cirrhosis caused by mitochondrial respiratory chain disorder

Shigehiro Enkai,[1] Sachi Koinuma,[2] Reiko Ito,[2] Junko Igaki,[3] Yukihiro Hasegawa,[3] Kei Murayama[4] and Akira Ohtake[5]

[1]*Department of Pediatrics, Fussa Hospital,* [2]*Division of Gastroenterology, National Center for Child Health and Development,* [3]*Division of Endocrinology and Metabolism, Tokyo Metropolitan Children's Medical Center, Tokyo,* [4]*Division of Metabolism, Chiba Children's Hospital, Chiba, and* [5]*Department of Pediatrics, Faculty of Medicine, Saitama Medical University, Saitama, Japan*

Abstract The patient had hepatomegaly with liver dysfunction at the age of 1 month. Magnetic resonance imaging performed at the age of 1 year showed multiple nodules of varying size in his liver. We were able to examine the mitochondrial respiratory chain function in the liver biopsy samples because all other differential diagnoses for hepatic cirrhosis had been ruled out. Complex I and IV activities were below the normal level (<30%) of the citrate synthase (CS) ratio. Liver blue native polyacrylamide gel electrophoresis showed an extremely weak complex I and IV band. Liver respiratory chain complexes I and IV were found to be deficient in this patient. The histologic findings were highly suggestive of mitochondrial respiratory chain disorder. Findings of progressive liver cirrhosis changes were observed in magnetic resonance imaging at the age of 5 years. An examination of the mitochondrial respiratory chain function should be performed along with a liver biopsy if mitochondrial respiratory chain disorder is suspected as a possible differential diagnosis of idiopathic hepatitis.

Key words chronic hepatitis, infant, liver cirrhosis, mitochondrial respiratory chain complex I and IV deficiency, mitochondrial respiratory chain disorder.

Mitochondrial respiratory chain disorder (MRCD), which is caused by the loss of one or more enzyme activities in respiratory chain complexes I–IV, has many clinical manifestations in various organs and is a known cause of mitochondrial encephalomyopathy, idiopathic hepatitis and idiopathic muscle weakness. Although MRCD is one of the differential diagnoses for hepatic disorder, it is not actively diagnosed. The early diagnosis of MRCD in the liver is important because some patients will subsequently develop liver cirrhosis or liver failure.[1,2] This report is based on a boy with chronic hepatic disorder and cirrhosis who was found to have mitochondrial respiratory chain complex I and IV deficiencies during his infant period.

Case Report

The patient was a Japanese boy born at term and weighing 3296 g; he was the second child of healthy parents with consanguinity. His elder sister (3 years old) is presently in good health. The mother's brother (31 years old) was found to have hepatic dysfunction during his infant period and his condition progressed to cirrhosis during adulthood. The proband's weight gain after birth was good. Jaundice and hepatomegaly were observed at the age of 1 month and he was admitted to our hospital. Upon admission (32 days after birth), he exhibited conjunctival icterus, his liver was palpable 5 cm below the right costal margin, he had normal muscle tone and no external malformations were noted. His laboratory data on admission showed cholestatic hepatitis. Tandem mass spectrometry, urine organic acid and bile acid analysis were normal. The following differential diagnoses were ruled out: autoimmune disease, infectious disease, disorder of organic acid metabolism and fatty acid oxidation, alpha 1-antitrypsin deficiency, tyrosinemia, galactosemia, and citrin deficiency. Furthermore, respiratory disorder, abnormal findings on skin or bone, and susceptibility to infection, which are the main symptoms of Langerhans cell histiocytosis and cystic fibrosis, are not present in this patient at the current age of 6 years. Imaging studies did not reveal any congenital portal venous or portal biliary tract malformations. The patient's transaminase (aspartate aminotransferase [AST] and alanine aminotransferase [ALT]) levels were 78–477 IU/l (AST) and 13–181 IU/l (ALT) and fluctuated with his physical condition. The patient's γ-GTP levels decreased to a normal range before the age of 6 months. Throughout the clinical course, the patient's blood lactate and pyruvic acid levels were almost always normal. Hypoglycemia was not observed during follow-up examinations. He exhibited normal growth and development. An abdominal magnetic resonance imaging (MRI) examination performed at the age of 2 months was normal except for hepatomegaly. However, an abdominal MRI performed at 1 year and 4 months showed multiple nodules of varying size in his liver, which appeared

Correspondence: Shigehiro Enkai, MD, Department of Pediatrics, Fussa Hospital, 1-6-1 Kamidaira, Fussa, Tokyo 197-0012, Japan. Email: enkai@fussahp.jp

Received 5 January 2012; revised 17 January 2013; accepted 19 February 2013.

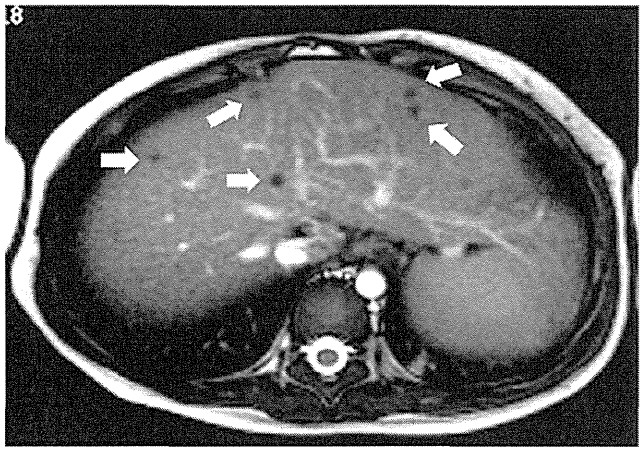

Fig. 1 Abdominal magnetic resonance image obtained at 1 year and 4 months shows multiple nodules (arrows) varying in size in the liver, which presented as a low-intensity area on T2-weighted imaging.

as low-intensity areas on T2-weighted images (see Fig. 1) and high-intensity areas on T1-weighted images without contrast enhancement. The number of nodules in his liver increased from the time of the MRI examination performed at the age of 1 year and 4 months. In addition, a transient elevation in the patient's serum ammonia levels (290 μg/dL) and impaired consciousness with the onset of fever and a poor appetite were observed at the age of 2 years. The clinical course during this episode showed positive results. Liver biopsies were performed during a laparotomy to inspect the progress of the liver cirrhosis at the age of 2 years and 1 month. He was suspected of having MRCD, which is one of the main causes of hepatic disorder, because all other differential diagnoses for hepatic cirrhosis had been ruled out. Thus, we were able to examine the mitochondrial respiratory chain function in the liver biopsy samples. Liver respiratory chain complexes I and IV were found to be deficient in this patient using both a respiratory chain enzyme assay (Table 1) and a liver blue native polyacrylamide gel electrophoresis (BN-PAGE).[3] Complex I and IV activities were below the normal level (<30%)[4] of the CS ratio. Liver BN-PAGE showed an extremely weak complex I and IV band in this patient. In addition, the rate of mtDNA and nDNA (quantitative polymerase chain reaction) was about 95.4% (normal level). Mitochondrial DNA depletion syndrome was ruled out. The macroscopic anatomy showed diffuse nodules on the surface of the liver. The microscopic findings for the liver are shown in Figure 2. Coenzyme Q, vitamin C, vitamin E, and carnitine therapy were initiated at an age of 2 years and 3 months. The patient continues to exhibit normal physical and mental development after diagnosis. His weight was 21.9 kg (+0.3SD score) and height was 117.5 cm (+0.6SD score) at the age of 6 years. However, the patient's transaminase levels were 56–311 IU/L (AST) and 31–174 IU/L (ALT), and findings of the follow-up MRI at the age of 5 years suggested progressive changes in liver cirrhosis. MRI demonstrated right lobe atrophy, enlargement of the left lobe, and an irregular edge border of the liver (Fig. 3a,b). MRI revealed a well-circumscribed mass 16 × 11-mm (see arrow) in liver segment VI (Fig. 3c). In addition to this mass, MRI demonstrated nodules 4–8 mm in size in the liver parenchyma, which were visualized as slightly hyperintense lesions on the T2-weighted images and as hypointensities on the T1-weighted images (Fig. 3c).

Table 1 Respiratory chain enzyme assay in the liver of the patient

	Complex I	Complex II	Complex III	Complex IV	CS
% of normal	14	37	62	15	54
CS ratio (%)	26	67	111	27	
Complex II ratio (%)	38		165	40	

Discussion

We reported a boy with chronic hepatic disorder and cirrhosis who was found to have mitochondrial respiratory chain complex I and IV deficiency during his infant period. In our experience, deficiencies of complexes I and IV account for about 15% of all diagnosed cases of MRCD in Japanese subjects. Nine clinical case reports of complex I and IV deficiencies, including adult subjects, were reported between 1988 and 2010. No specific manifestations of complex I and IV deficiency were observed in the past reports. The patient's blood lactate/pyruvate rate was almost normal in the clinical course. However, a normal lactate level does not exclude respiratory chain defects in MRCD, including mitochondrial hepatopathy.[5,6] The molecular and genetic causes of complex I and IV deficiency are not clear.

The histological findings of liver biopsy specimens from patients with primary mitochondrial hepatopathies reveal individual, non-specific histologic and ultrastructural findings, with predominant microvesicular steatosis and canalicular cholestasis.[7] Periportal and centrilobular fibrosis are characteristic features, and the dropout of broad bands of hepatocytes leads to micronodular cirrhosis.[7] Thus, the histologic findings of this case were highly suggestive of MRCD. In addition, if electron micrographs revealed morphological abnormality of mitochondria in liver biopsies, they would have been useful for confirming diagnosis of MRCD.

With respect to MRI findings, nodules which were found at the age of 1 year were not detected at the age of 5 years. The nodules in Figure 1 might be regenerative nodules (RN) associated with hepatic cirrhosis, because RN typically appear as hypointense lesions on T2-weighted images[8] and the imaging findings at the age of 5 years were typical of hepatic cirrhosis. Furthermore, focal nodular hyperplasia, which is one of the important differential diagnoses of hepatic nodules in infants, was excluded on the basis of the high signal intensity in the non-enhanced T2-weighted images.[9] However, these nodules were so small that they were difficult to evaluate by MRI or histopathology.

Findings of progressive liver cirrhosis changes were observed in a liver MRI at the age of 5 years (Fig. 3a–c). The 16 × 11-mm mass in Figure 3c (see arrow) was visualized as a hyperintensity on opposed-phase T1-weighted gradient-echo images and as a slightly low-intensity area on the T2-weighted images. Focal

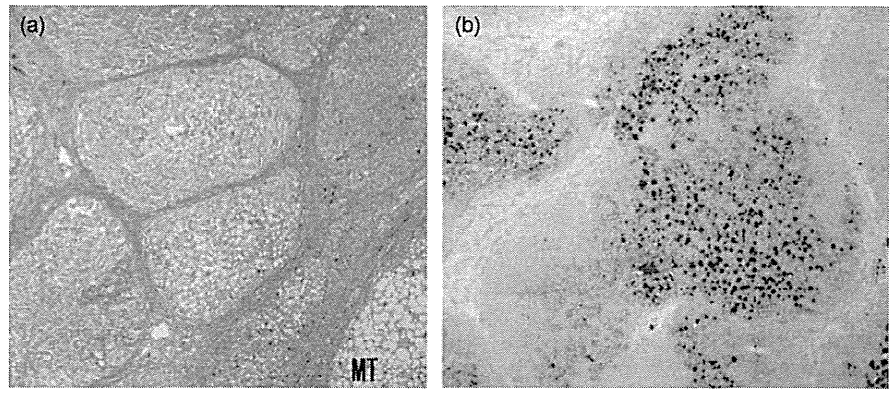

Fig. 2 (a) Masson trichrome stain: Microscopic findings in the liver show the division of a hepatic lobule into nodules by bridging fibrosis in the liver tissue. (b) Sudan III stain: Liver tissues show heterogeneous hepatic steatosis in each septum. Portal fibrosis was observed in liver tissues without inflammation (not shown).

nodular hyperplasia was excluded because the mass did not show the high-intensity on the non-enhanced T2-weighted images. The size remained unchanged as compared to the previous year. Thus, the mass was suspected to be a regenerative nodule or adenomatous hyperplasia, associated with hepatic cirrhosis. In addition to this mass, MRI in Figure 3c demonstrated nodules 4–8 mm in size in the liver parenchyma. Although these nodules were found to contain lipids inside, as they were visualized as low-intensity areas on opposed-phase T1-weighted gradient-echo images and as high-intensity areas on in-phase images, they were too small to evaluate in detail.

The early and accurate diagnosis of MRCD is important because appropriate therapy and guidance can be provided to the patient and his/her family before the condition worsens. MRCD is difficult to diagnose because the clinical manifestations do not depend on the type of complex deficiency. Some previous patients have died of hepatic failure during the neonatal period or infancy, while other patients never develop hepatic disease despite long-term follow-up observation.[1] However, it is conceivable that a regular screening for secondary liver cancer is necessary for the patient with progressive cirrhosis, along with MRCD during his infant period.[10]

With respect to diagnosis, regular ultrasound or CT examinations are needed for infants with idiopathic chronic hepatitis because multiple nodules in the liver gradually appeared in the patient. Furthermore, we conclude that an examination of the mitochondrial respiratory chain function should be performed along with a liver biopsy if MRCD is suspected as a possible differential diagnosis of idiopathic hepatitis under the signs of liver cirrhosis, as in this case.

Acknowledgments

The authors report no conflicts of interest. We have no disclosures to make and have not received any financial support.

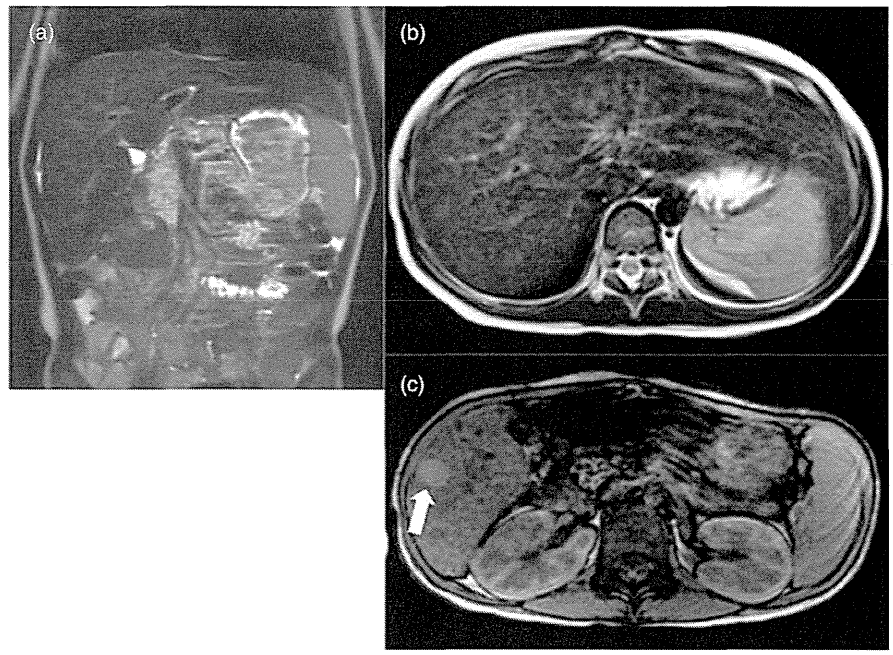

Fig. 3 (a) T2-weighted magnetic resonance image (MRI) demonstrates right lobe atrophy, enlargement of the left lobe, and an irregular edge border of the liver at the age of 5 years. (b) T2-weighted MRI shows marked hyperintensity in the periportal region. The hepatic parenchyma appears heterogeneously enhanced in the delayed phase. (c) T1-weighted MRI revealing a well-circumscribed 16 × 11-mm mass (see arrow) in liver segment VI. This mass is visualized as a hyperintensity on opposed-phase T1-weighted gradient-echo images and as a slightly lower-intensity area on the T2-weighted images. In addition to this mass, MRI demonstrates nodules 4–8 mm in size in the liver parenchyma, which are visualized as slightly hyperintense lesions on the T2-weighted images and as hypointensities on the T1-weighted images.

References

1 Carcia-cazorla A, De Lonlay P, Rustin P *et al.* Mitochondrial respiratory chain deficiencies expressing the enzymatic deficiency in the hepatic tissue: a study of 31 patients. *J. Pediatr.* 2006; **149**: 401–5.

2 Lee WS, Sokol RJ. Mitochondrial hepatopathies: advances in genetics and pathogenesis. *Hepatology* 2007; **45**: 1555–65.

3 Schagger H, Aquila H, von Jagow G. Coomassie blue-sodium dodecyl sulfate- polyacrylamide gel electrophoresis for direct visualization of polypeptides during electrophoresis. *Anal. Biochem.* 1988; **173**: 201–55.

4 Bernier FP, Boneh A, Dennett X, Chow CW, Cleary MA, Thorburn DR. Diagnostic criteria for respiratory chain disorders in adults and children. *Neurology* 2002; **59**: 1406–11.

5 Kirby MD, Crawford M, Cleary MA, Dahl HH, Dennet X, Thorburn DR. Respiratory chain complex I deficiency: an underdiagnosed energy generation disorder. *Neurology* 1999; **52**: 1255–64.

6 Fellman V, Kotarsky H. Mitochondrial hepatopathies in the newborn period. *Semin. Fetal Neonatal Med.* 2011; **16**: 222–8.

7 Suchy FJ, Sokol RJ, Balistreri WF. *Liver Disease in Children*, 3rd edn. Cambridge University Press, Cambridge, 2007; 803–29.

8 Hussain SM, Terkivatan T, Zondervan PE *et al.* Focal nodular hyperplasia: Findings at state-of-the-art MR imaging, US, CT, and pathologic analysis. *Radiographics* 2004; **24**: 3–17.

9 Hanna RF, Aguirre DA, Kased N, Emery SC, Peterson MR, Sirlin CB. Cirrhosis-associated hepatocellular nodules: correlation of histopathologic and MR imaging features. *Radiographics* 2008; **28**: 747–69.

10 Scheers I, Bachy V, Stephenne X, Sokal EM. Risk of hepatocellular carcinoma in liver mitochondrial respiratory chain disorders. *J. Pediatr.* 2005; **146**: 414–7.

Endoplasmic Reticulum Stress and Apoptosis Contribute to the Pathogenesis of Dominantly Inherited Isolated GH Deficiency Due to *GH1* Gene Splice Site Mutations

Daisuke Ariyasu, Hiderou Yoshida,* Makoto Yamada, and Yukihiro Hasegawa*

Department of Endocrinology and Metabolism (D.A., Y.H.), Tokyo Metropolitan Children's Medical Center, Tokyo 183–8561, Japan; Department of Biochemistry and Molecular Biology (H.Y.), Graduate School of Life Science, University of Hyogo, Hyogo 678–1297, Japan; and Department of Pharmacy (M.Y.), Tokyo University of Science, Tokyo 162–0825, Japan

Dominantly inherited isolated GH deficiency is mainly caused by a heterozygous donor site mutation of intron 3 in the *GH1* gene. An exon 3 deletion in GH (del32–71 GH) is produced from a mutant allele, whereas wild-type GH is produced from the other allele. Several studies have demonstrated a dominant negative effect of del32–71 GH on wild-type GH secretion, but the precise molecular mechanisms remain unclear. We hypothesized that unfolded del32–71 GH accumulates in the endoplasmic reticulum (ER) and causes ER stress and apoptosis in somatotrophs, promoting GH deficiency. To evaluate del32–71 GH–mediated ER stress, we established GH4C1 cell lines with doxycycline (dox)-controlled del32–71 GH expression. In 20 of 23 dox-controlled cell lines, the concentration of wild-type GH in the culture medium significantly decreased with del32–71 GH induction, demonstrating the dominant negative effect of this mutant. Cell viability, mRNA abundance of ER stress-response genes, caspase activation, and DNA fragmentation were evaluated in 5 dox-controlled cell lines selected as cellular models. In 4 of the 5 cell lines, del32–71 GH induction decreased cell viability, increased expression of 3 major ER stress response pathways (PRKR-like endoplasmic reticulum kinase [PERK], activating transcription factor-6 [ATF6], and inositol requirement 1 [IRE1]), and induced caspase-3 and caspase-7 activation. In 1 of the 4 cell lines, DNA fragmentation was demonstrated. Finally, overexpression of XBP1(S), a nuclear transcription factor downstream of IRE1, completely reversed the observed caspase activation. These data suggested that del32–71 GH–mediated ER stress and apoptosis contributed to the decrease in wild-type GH secretion observed in GH deficiency due to the *GH1* gene slice-site mutations. (***Endocrinology* 154: 3228–3239, 2013)**

Dominantly inherited isolated GH deficiency is mainly caused by heterozygous donor-site mutations of intron 3 in the *GH1* gene (1, 2). Such splice-site mutations cause in-frame mRNA skipping of exon 3, corresponding to amino acids 32 to 71. As a result, a 17.5-kDa exon 3 deletion-mutant GH protein (del32–71 GH) is produced from the mutant allele. The GH transcript from the other wild-type allele includes exons 1 to 5 and produces a 22-kDa wild-type GH protein. One wild-type *GH1* allele appears to be sufficient to maintain a serum concentration of wild-type GH within the normal range because children harboring a deletion in just one *GH1* allele exhibit a normal stature (3). However, patients with the splice-site mutations have low serum concentrations of wild-type GH, despite the presence of one wild-type *GH1* gene. Thus, it has been suggested that del32–71 GH exerts a dominant negative effect on the secretion of wild-type GH, but the precise molecular mechanisms involved have remained

ISSN Print 0013-7227 ISSN Online 1945-7170
Printed in U.S.A.

Received March 17, 2013. Accepted May 29, 2013.
First Published Online June 4, 2013

* H.Y. and Y.H. contributed equally to the study.

Abbreviations: ATF6, activating transcription factor-6; dox, doxycycline; EM, electron microscopy; ER, endoplasmic reticulum; ERAD, endoplasmic reticulum–associated degradation; IRE1, inositol requirement 1; IRMA, immunoradiometric assay; PERK, PRKR-like endoplasmic reticulum kinase; q, quantitative.

elusive. It has been speculated that del32–71 GH lacks the loop connecting helix 1 and helix 2 (4), and, therefore, the protein cannot be properly folded in the endoplasmic reticulum (ER) (5, 6). In addition, one study has shown that unfolded del32–71 GH interferes with the wild-type GH secretory pathway by destroying secretory vesicles (7).

Proteins are synthesized and folded in the ER, and only correctly folded proteins are transported to the Golgi apparatus. Proteins judged as "unfolded" in the ER are (1) suppressed at the translational level, (2) refolded by ER chaperones, or (3) degraded by the proteasome via endoplasmic reticulum–associated degradation (ERAD) machinery. In mammals, these 3 cell-protective responses are executed through the PRKR-like endoplasmic reticulum kinase (PERK), activating transcription factor-6 (ATF-6), and inositol requirement 1 (IRE1) pathways, respectively (8–11). These self-defense mechanisms in eukaryotic cells, which function to alleviate the stress caused by unfolded proteins, are collectively referred to as the ER stress responses. When cells synthesize unfolded proteins in amounts that exceed the capacity of the self-defense mechanisms, an apoptotic pathway is triggered to ensure survival of the organism as the last line of defense (12). ER stress has a significant role in the development of several diseases, such as Alzheimer disease, Parkinson disease, type 2 diabetes, familial central diabetes insipidus, and Wolfram syndrome (13–18).

Based on these previous studies, we hypothesized that ER stress, caused by unfolded del32–71 GH accumulating in the ER, may be one of the factors involved in the development of GH deficiency due to the splice site mutations. Involvement of ER stress in the dominant negative effect of del32–71 GH has been speculated to be unlikely in 2 studies (5, 7). However, these 2 studies did not evaluate ER stress using cells expressing both human wild-type and del32–71 GH; the former study (5) performed transient expression of del32–71 GH to COS cells, and the latter study (7) stably expressed del32–71 GH to rat GC cells. Thus, we tried to analyze the involvement of ER stress using cells stably expressing human wild-type and del32–71 GH.

In this study, in vitro data indicated that del32–71 GH caused ER stress and apoptosis in GH4C1 rat pituitary cells. Using a doxycycline (dox)-inducible gene expression system, we established double-transfected stable GH4C1 cell lines in which wild-type GH was constantly expressed and del32–71 GH expression was induced. Using 5 cell lines chosen as a cellular model of this disorder, we demonstrated that the induction of del32–71 GH caused ER stress, leading to apoptosis of the cells.

Materials and Methods

Isolation of wild-type GH1 cDNA and del32–71 GH1 cDNA

Wild-type and del32–71 GH1 cDNA sequences were amplified from a pituitary cDNA library by standard PCR methods using a sense primer that includes the initiation codon and an antisense primer that includes the termination codon. The initial PCR product was subjected to electrophoresis on a 1% agarose gel, and regions around 670 and 550 bp, corresponding with the PCR products of wild-type and del32–71 GH1 cDNA, respectively, were separately isolated and purified. The 550-bp PCR product was amplified by a second PCR using the same primers. The second PCR product was purified, and the deletion of exon 3 was confirmed by direct sequencing.

Expression vectors

For preparation of constructs for the dox-inducible gene expression system, we employed the Tet-Off Advanced Doxycycline Inducible Gene Expression System (Clontech Laboratories, Mountain View, California). First, wild-type *GH1* cDNA was inserted into the pcDNA3.1-Hygro(+) vector (Invitrogen, Carlsbad, California) using NheI and ApaI restriction enzymes (pcDNA3.1–wild-type GH). Regions containing the cytomegalovirus promoter, wild-type *GH1* cDNA sequence, and polyadenine signal were isolated from pcDNA3.1–wild-type GH using standard PCR methods and inserted into the Tet-Off Advanced Vector (supplied with the kit) via a HindIII restriction site in the 5′ to 3′ direction (Tet-Off advanced–wild-type GH). del32–71 GH1 cDNA was inserted into the pTRE–Tight Vector (supplied with the kit) via KpnI and HindIII restriction sites (pTRE–del32–71 GH). For preparation of GFP-XBP1(S) expression constructs, the rat *XBP1(S)* cDNA sequence was amplified and purified from mRNA of thapsigargin-treated GH4C1 cells by RT-PCR and inserted into the pTagGFP2-C vector (Evrogen, Moscow, Russia) using XhoI and KpnI restriction enzymes [GFP-XBP1(S)]. All primers sequences used in this study are listed in Supplemental Table 1 published on The Endocrine Society's Journals Online web site at http://endo.endojournals.org.

Cell culture

GH4C1 rat pituitary cells, which are known to secrete little rat GH, were purchased from American Type Culture Collection (Manassas, Virginia). GH4C1 cells were cultured in Ham's F-10 medium, 15% horse serum, and 2.5% fetal bovine serum (both sera were not heat-inactivated). Endogenous rat GH was confirmed to be absent from the culture medium by immunoblotting with human anti-GH antibodies (Dako, Carpinteria, California) and RT-PCR.

Transfection

Lipofectamine reagent (Invitrogen) and Lipofectamine Plus reagent (Invitrogen) were used for transfections. Transfections were performed according to the manufacturer's instructions 48 hours after seeding at a density of 5×10^5 cells per 2 mL of medium in 6-well culture plates.

Establishment of stable cell lines using a dox-inducible gene expression system

GH4C1 cells were transfected with Tet-Off advanced wild-type GH (explained above). Culture medium containing 0.4 mg/mL G418 (Promega, Madison, Wisconsin) was exchanged every 3 days. Each surviving cell line was transiently transfected with pTRE–Tight Luc vector (supplied with the kit) in the presence or absence of 100 ng/mL dox (supplied with the kit), and fold inductions (−dox/+dox) of luciferase activity were calculated. Expression of human wild-type GH and fold induction of luciferase activity were evaluated among all 40 stable cell lines by immunoblotting and luciferase assays, respectively, and only 1 of these 40 cell lines was chosen. Next, the cell line was transfected with pTRE–del32–71 GH and hygromycin marker (supplied with the kit) with a molar ratio of 20:1 in the presence of 100 ng/mL dox. Culture medium containing 100 ng/mL dox, 0.4 mg/mL G418, and 0.2 mg/mL hygromycin (Invitrogen) was exchanged every 3 days. Individual double-transfected stable cell lines were evaluated for expression of wild-type GH and del32–71 GH in the presence or absence of 100 ng/mL dox by quantitative (q) RT-PCR and immunoblotting.

RT-PCR and qRT-PCR

Total RNA (500 ng) was extracted using RNAiso Plus (Takara, Tokyo, Japan) and then converted to cDNA using PrimeScript RT Master Mix (Takara). The aliquot of cDNA was used for RT-PCR and qRT-PCR. A Taq polymerase, KOD-FX (Toyobo, Osaka, Japan), was used for standard PCR and RT-PCR, and SYBR Premix Ex Taq II (Takara) was used for qRT-PCR.

qRT-PCR was performed using a Thermal Cycler Dice Real Time System (Takara). The amplification conditions consisted of 1 cycle at 95°C for 30 seconds and 35 cycles at 95°C for 5 seconds and 60°C for 30 seconds. Dissociation curve analyses were performed at conditions of 95°C for 15 seconds, 60°C for 30 seconds, and 95°C for 15 seconds. The relative concentrations of mRNAs were calculated using the standard curve and normalized to β-actin expression.

Evaluation of ER stress response gene transcript

The relative abundance of ER stress response gene transcripts was evaluated by qRT-PCR. As ER stress response genes, *GADD34*, *CHOP*, *BiP*, *GRP94*, and *XBP1* were chosen in this study. BiP and XBP1 were also used as ER stress markers for the purpose of screening cell lines with dox-controlled del32–71 GH expression. BiP is an ER chaperone downstream of ATF6 that enhances folding capacities in the ER and XBP1 is a transcription factor downstream of IRE1 that activates transcription of ERAD components (12).

SDS-PAGE and immunoblotting

SDS-PAGE and immunoblotting were performed using 15% polyacrylamide gels, polyvinylidene difluoride membranes, and ECL Plus detection reagent (Amersham, Little Chalfont, Buckinghamshire, England) according to standard procedures (19).

In soluble/insoluble fraction assays, cells cultured in 60-mm dishes were scraped, suspended in 50 μL of 1% Triton X-100 in PBS, and incubated at 4°C for 15 min. The lysates were centrifuged at 17 800 *g* for 5 min, and the supernatants and precipitates were isolated in separate microfuge tubes. Next, 16.7 μL of 4× sample buffer (0.1 mM Tris-HCl, pH 6.8, containing 4% SDS, 20% sucrose, 0.01% bromophenol blue, and 10% 2-mercaptoethanol) was added to each supernatant, and 50 μL of radioimmunoprecipitation assay buffer (10 mM Tris-HCl, pH 7.4, containing 5 mM EDTA, 0.1% SDS, and 1% Triton X-100) plus 16.7 μL of 4× sample buffer was added to each precipitate. Supernatants and precipitates were heated at 100°C for 5 minutes and centrifuged at 17 800 *g* for 15 minutes at 4°C. Aliquots of the resulting supernatants were loaded onto 15% polyacrylamide gels.

Measuring the GH concentration in culture medium

Cell lines with dox-controlled del32–71 GH expression were seeded at a density of 2.5×10^4 cells/150 μL of culture medium into 96-well culture plates in the presence or absence of 100 ng/mL dox. Forty-eight hours later, 100 μL of culture medium was collected from each cell line and mixed with 400 μL of PBS. The GH concentration was subsequently measured by a commercially available immunoradiometric assay (IRMA) using a GH measuring kit (Daiichi; TFB, Tokyo, Japan). We confirmed that del32–71 GH was absent from this assay; a concentration of del32–71 GH in MG132-treated near-confluent GH4C1 cell lysates transfected with del32–71 GH was below the detectable limit. The measurement range for IRMA was 0.05 to 25 ng/mL. Both intra- and interassay coefficients of variation were less than 3%.

Cell viability

Cell lines with dox-controlled del32–71 GH expression were seeded at a density of 2.5×10^4 cells/150 μL of medium into 96-well culture plates in the presence or absence of 100 ng/mL dox. Forty-eight hours after seeding, 10% CCK-8 reagent (Dojindo, Kumamoto, Japan) was added with fresh culture medium. Absorbance was measured 4 hours later using a multiplate reader. The CCK-8 reagent contained a water-soluble disulfonated tetrazolium salt that was reduced by NADH to produce the corresponding formazan dye (absorbance at 460 nm). CCK-8 reagent has been used as a chromogenic indicator for NADH and cell viability (20).

DNA fragmentation assay

To assess DNA ladder formation, low–molecular-weight DNA was extracted from 2×10^6 cells using the ApoLadder EX Kit (Takara). Extracted DNA fragments were applied to 2% agarose gels, separated electrophoretically, and visualized with GelRed (Wako Chemicals, Irvine, California).

Reagents for the pharmacological induction of ER stress, proteasome inhibition, and lysosome inhibition

Thapsigargin (Sigma-Aldrich, St Louis, Missouri), the proteasome inhibitor MG132 (Peptide Institute, Osaka, Japan), and chloroquine (Sigma-Aldrich) were added to the culture medium 16 hours before harvesting at final concentrations of 1 μM, 10 μM, and 50 μg/mL, respectively.